Fig. 1 Tumor cells are arranged in small clusters divided by thin fibrous connective tissue septa. Tumor cells show abundant eosinophilic granular cytoplasm with numerous coarse granules. (Hematoxylin and eosin (H&E) stain, original magnification ×100). Inset: mitotic figure is present. (H&E stain, original magnification ×400)

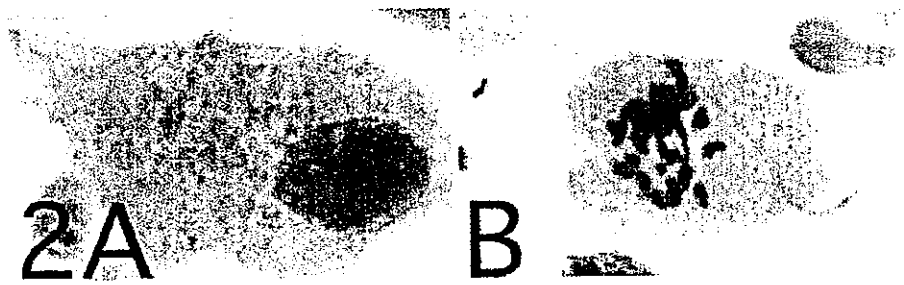

Fig. 2 Tumor cells obtained from the resected tumor showed increased nuclear to cytoplasmic ratio, abundant acidophilic granular cytoplasm with numerous coarse granules, and hyperchromatic coarse nuclei with large nucleoli (A). Mitotic figure is present (B). (Papanicolaou-stain, original magnification ×1000)

morphism. Electron microscopically, the cytoplasm of the tumor cells was abundant, with numerous lysosomes. On Papanicolaou-stained smears obtained from the resected tumor, tumor cells showed abundant acidophilic granular cytoplasm with a lot of coarse granules positive for diastase-resistant periodic acid-Schiff (PAS) reaction, increased nuclear to cytoplasmic (N/C) ratio, pleomorphic nuclei with hyperchromasia and coarse chromatin, large nucleoli throughout the cytological sample (Fig. 2A) and immunoreactivity for S100 protein. Some multi-nucleate tumor cells and mitotic figures were also seen (Fig. 2B). The patient developed bilateral pleural effusion 4 years after the surgical resection. Aspiration preparations obtained from the pleural effusion revealed tumor cells similar to those seen in smears obtained from the resected tumor, and the tumor cells were immunoreactive for S-100 protein. A CT scan of his abdomen showed multiple nodular lesions in his liver, which had not been seen on the CT scan done before the esophagogastrectomy. The biopsy from the nodular lesions in his liver was not done, and metastasis of the granular cell tumor to the liver was clinically assumed. The patient died of respiratory failure 4 months later. Autopsy was not done.

The present tumor had characteristic morphological and immunohistochemical features, indicating a granular cell tumor. Thus, the tumor cells had abundant acidophilic granular cytoplasm with diastase-resistant PAS-positive lysosomal granules. Immunohistochemically, the tumor cells were positive with markers indicative for granular cell tumors: S-100 protein, keratan sulfate, CD57, vimentin, NSE and CD68 [7]. Negative staining of endocrine markers and myogenic markers was helpful to differentiate this tumor from endocrine tumors or myogenic tumors [7]. This tumor was also different from gastrointestinal stromal tumor on the basis of negative staining for CD34 and c-kit and from peripheral nerve sheath tumor on the basis of positive reaction for keratan sulfate [2, 7].

Granular cell tumor is generally a benign tumor occurring in any part of the body [7]. Malignant granular cell tumor is extremely rare, estimated to be 1–2% of all cases [7]. Four cases of malignant esophageal granular cell tumor have been reported [1, 5, 6, 9]. Crawford and DeBakey reported a case of 31-year-old female patient with infiltration into the trachea and thyroid cartilage [1]. The 23-year-old female patient reported by Obiditsch-Mayer and Salzer-Kuntschik had prominent tracheal and esophageal infiltration, as well as metastases to the cervical lymph nodes, and died 7 months later [5]. Ohmori et al. reported a 70-year-old female patient with malignant granular cell tumor with mitotic figures [6]. Wyatt et al. reported a 78-year-old female patient with malignant granular cell tumor with mitotic figures and vascular invasion [9]. Recently, Fanburg-Smith et al.

proposed histological criteria to define malignant granular cell tumor of the soft part, including necrosis, spindling, vesicular nuclei with lager nucleoli, increased mitotic activity (>2 mitosis/10 high power fields at ×200 magnification) and a high N/C ratio and pleomorphism [3]. They classified the granular cell tumors that satisfy three or more of these criteria as histologically malignant granular cell tumors. More recently, Wieczorek et al. proposed cytological features of malignant granular cell tumor of the soft part, including hyperchromasia, coarse chromatin, increased N/C ratio, nuclear pleomorphism and vesicular nuclei with enlarged nucleoli and spindle cell morphology, which were associated the most closely with malignancy when they were present throughout the cytological sample [8]. They also reported that mitoses were present in malignant granular cell tumors and absent from all benign granular cell tumors [5]. The present case satisfies five of these criteria, including necrosis, spindling, vesicular nuclei with large nucleoli, increased mitotic activity and pleomorphism. In addition, the present case developed pleural dissemination and assumed metastasis to the liver and is, therefore, considered a true malignant form of this generally benign tumor [4]. In the present case, the presence of round to oval shaped tumor cells with small blunt nuclei proliferating in the lamina propria just beneath the esophageal epithelium suggests the possibility of malignant transformation of a preexisting benign granular cell tumor.

Acknowledgements We thank Dr. Kaiyo Takubo, Department of Clinical Pathology, Tokyo Metropolitan Institute of Gerontology, Tokyo, and Professor David Y. Graham, Baylor College of Medicine, Houston, TX, for their helpful comments and encouragement.

References

1. Crawford ES, DeBakey ME (1953) Granular-cell myoblastoma: two unusual cases. Cancer 6:786–789
2. Ehara T, Katsuyama T (1990) Characterization of glycoconjugates found in granular cell tumors, with special reference to keratan sulfate. Virchows Arch 58:221–227
3. Fanburg-Smith JC, Meis-Kindblom JM, Fante R, Kindblom LG (1998) Malignant granular cell tumor of soft tissue: diagnostic criteria and clinicopathologic correlation. Am J Surg Pathol 22:779–794
4. Johnston MJ, Helwig EB (1981) Granular cell tumors of the gastrointestinal tract and perianal region. A study of 74 cases. Dig Dis Sci 26:807–816
5. Obiditsch-Mayer I, Salzer-Kuntschik M (1961) Malignes, "getorntzelliges neurom" sogenanntes, "myoblastenmyom," des oesophagus. Beitr Pathol Anat 125:357–373
6. Ohmori T, Arita N, Uraga N, Tabei R, Tani M, Okamura H (1987) Malignant granular cell tumor of the esophagus. A case report with light and electron microscopic, histochemical, and immunohistochemical study. Acta Pathol Jpn 37:775–783
7. Ordonez NG (1999) Granular cell tumor: a review and update. Adv Anat Pathol 6:186–203
8. Wieczorek TJ, Krane JF, Domanski HA, Akerman M, Carlen B, Misdraji J, Granter SR (2001) Cytologic findings in granular cell tumors, with emphasis on the diagnosis of malignant granular cell tumor by fine-needle aspiration biopsy. Cancer 93:398–408
9. Wyatt MG, O'Donoghue DS, Clarke TJ, Teasdale C (1991) Malignant granular cell tumour of the oesophagus. Eur J Surg Oncol 17:388–391

ELSEVIER

Neoplasm

SYMMETRIC DUMBBELL GANGLIONEUROMAS OF BILATERAL C2 AND C3 ROOTS WITH INTRADURAL EXTENSION ASSOCIATED WITH VON RECKLINGHAUSEN'S DISEASE: CASE REPORT

Kazuhiko Kyoshima, M.D.,* Keiichi Sakai, M.D.,* Miki Kanaji, M.D.,* Susumu Oikawa, M.D.,* Sumio Kobayashi, M.D.,* Atsushi Sato, M.D.,* and Jun Nakayama, M.D.†

**Departments of Neurosurgery and †Laboratory Medicine, Shinshu University School of Medicine, Matsumoto, Japan*

Kyoshima K, Sakai K, Kanaji M, Oikawa S, Kobayashi S, Sato A, Nakayama J. Symmetric dumbbell ganglioneuromas of bilateral C2 and C3 roots with intradural extension associated with von Recklinghausen's disease: case report. Surg Neurol 2004;61: 468–73.

BACKGROUND

Ganglioneuromas are rare benign tumors arising most commonly from the sympathetic nervous system. They occasionally grow in a dumbbell fashion extending into the spinal canal extradurally. However, ganglioneuromas of the cervical spine with intradural extension or multiple locations or in association with von Recklinghausen's disease are rare.

CASE DESCRIPTION

A 35-year-old man with von Recklinghausen's disease presented with tetraparesis and respiratory dysfunction. Preoperative neuroimaging revealed an intradural mass extending from the foramen magnum to the C4 vertebral level, as well as bilateral extravertebral extension connecting it with bilateral paraspinal lesions in a dumbbell fashion. Four intradural tumors associated with the bilateral C2 and C3 nerves and located ventrally were removed, leaving the intraforaminal and extradural portion intact. The procedure resulted in postoperative symptomatic improvement. Second, extravertebral tumors of the left neck, which were not related to the cervical sympathetic nerve, were removed. The pathologic diagnosis of the tumors of both the intradural space and cervical neck was ganglioneuroma.

CONCLUSION

We present an extremely rare case in an adult with von Recklinghausen's disease who had bilateral, symmetric and multiple dumbbell ganglioneuromas with intradural extension, and also multiple bilateral ganglioneuromas at the neck. The intradural ganglioneuromas were suspected to have originated from the posterior root ganglions of the bilateral C2 and C3 nerves and to have extended ventrally to the spinal cord involving not only sensory but also motor rootlets; the ganglioneuroma of the neck was suspected to have originated from the cervical nerve itself.

KEY WORDS

Cervical spine, dumbbell tumor, ganglioneuroma, intradural extension, spinal neoplasm, von Recklinghausen's disease.

Ganglioneuromas are rare, slow-growing benign tumors in children or young adults arising from tissues of the neural crest, most commonly from the sympathetic nervous system. They occasionally grow in a dumbbell fashion extending into the spinal canal extradurally. However, ganglioneuromas located in the cervical spine originating from the sensory ganglion or nerve, extending intradurally, or occurring in multiple locations are extremely uncommon. Association with von Recklinghausen's disease has also rarely been reported. We present a case of multiple dumbbell ganglioneuromas of the cervical spine with intradural extension associated with von Recklinghausen's disease.

Address reprint requests to: Dr. Kazuhiko Kyoshima, Department of Neurosurgery, Shinshu University School of Medicine, Asahi 3-1-1, Matsumoto 390–8621, Japan.

Received December 12, 2002; accepted April 28, 2003.

0090-3019/04/$–see front matter
doi:10.1016/S0090-3019(03)00393-8

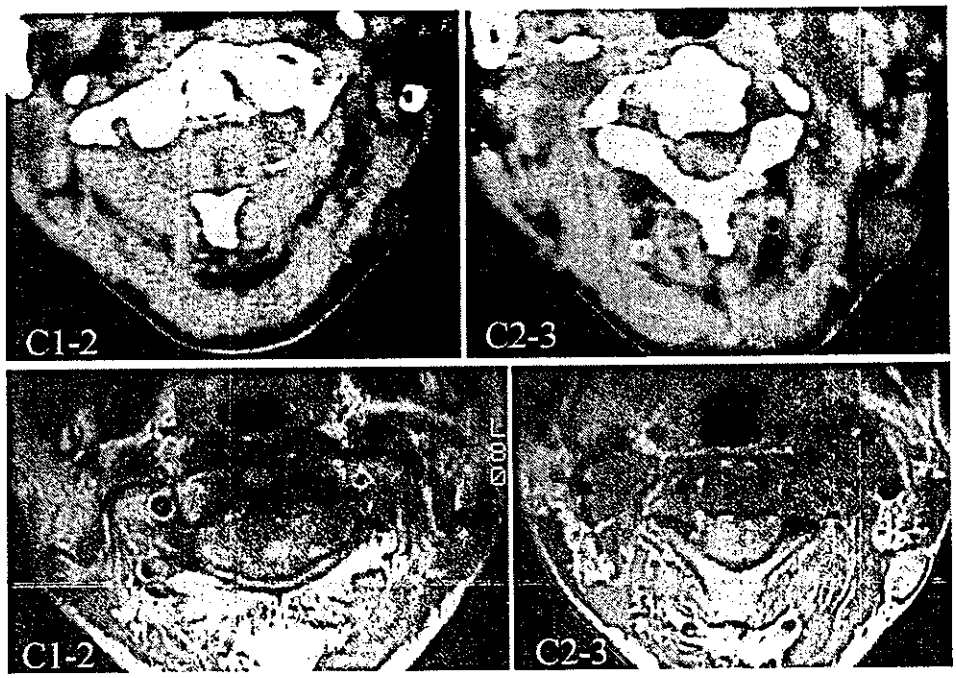

1 Transverse sections of preoperative plain computerized tomography scan (upper) and enhanced magnetic resonance imaging (lower) demonstrating an intraspinal dumbbell shaped mass extending to the bilateral paraspinal regions at the C1–2 level and through the C2–3 intervertebral foramina.

CASE REPORT

A 35-year-old man with a 3-year history of numbness in the right hand was hospitalized because of progressive gait disturbance and clumsiness of both hands 1 year before admission. Preoperative examination showed mild tetraparesis and slight respiratory dysfunction, as well as a number of subcutaneous nodules and café au lait spots over the patient's neck and face. Chromosomal analysis did not demonstrate any abnormalities. Plain X-ray and neuroimaging revealed enlargement of the bilateral C2-C3 intervertebral foramina and an intradural extramedullary mass lesion extending from the foramen magnum to the C4 vertebral level and compressing the spinal cord posteriorly. The mass, which was continuous with bilateral extravertebral components at the C1-C2 level and through the C2-C3 intervertebral foramina, showed low density without enhancement on computerized tomography scanning and low intensity with slight heterogeneous enhancement on magnetic resonance imaging (Figures 1 and 2). Vertebral angiography showed no abnormalities.

The patient underwent a suboccipital partial craniectomy and wide laminectomy of C1 to C4. The intradural mass, which preoperative magnetic resonance imaging (MRI) had demonstrated as 1 unit, in fact consisted of 4 bilateral C2 and C3 root-related tumors located ventrally to the spinal cord (Figure 3, left and middle). All these tumors involved both sensory and motor rootlets except for the right C3-related tumor, which involved the sensory rootlets alone (Figure 3, middle). The tumors were solid, smooth, and elastic without apparent adhesion to each other or the spinal cord, and were pulled out after debulking without causing avulsion of the motor nerve rootlets because these rootlets were elongated and tortuous (Figure 3, middle). The tumors, which showed little vascularization, were amputated at the dural side, and no attempt was made to remove the intraforaminal or extradural portion. This means that all the nerve rootlets of bilateral C2 and C3, except for the right C3 motor rootlets, were resected. Postoperatively the patient showed improvement of manual clumsiness and respiratory dysfunction but persistent hypesthesia of left C2 dermatome. At the second operation the extravertebral tumors of the left neck, which were not related to the cervical sympathetic nerve, were removed leaving the intraforaminal part intact. Three solid and elastic tumors were found between the carotid artery and jugular vein. The tumor arising from the C2 cervical nerve was isolated from the C2 root-related dumbbell tumor; the tumor of the C3 cervical nerve extended into the C2-C3 intervertebral foramen and was suspected of being connected with the intradural mass; and the tumor of the C4 cervical nerve extended into the C3-C4 ver-

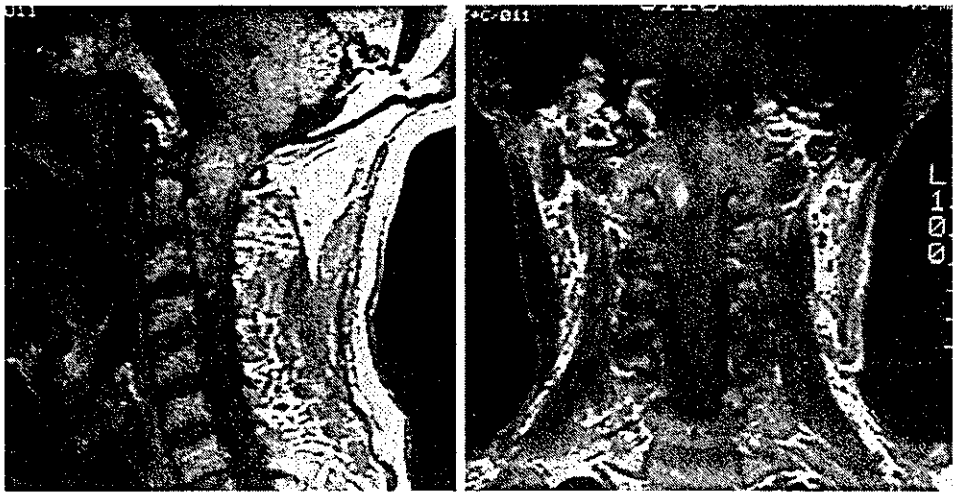

2 Preoperative enhanced magnetic resonance imaging. **Left:** Sagittal imaging revealing an intradural extramedullary mass with slight heterogeneous enhancement extending from the foramen magnum to the C4 vertebral level and compressing the spinal cord posteriorly. **Right:** Coronal imaging demonstrating bilateral extension of the intraspinal mass through C2–3 intervertebral foramina in dumbbell fashion.

tebral foramen, where no intradural mass had been observed during the previous surgery (Figure 3, right). Postoperatively, a chest X-ray film showed slight paresis of the left diaphragm but no change in the respiratory function. The patient showed no further neurologic deficit except hypesthesia from the mandibular area to the shoulder on the left side. The pathologic diagnosis of the tumors of both the

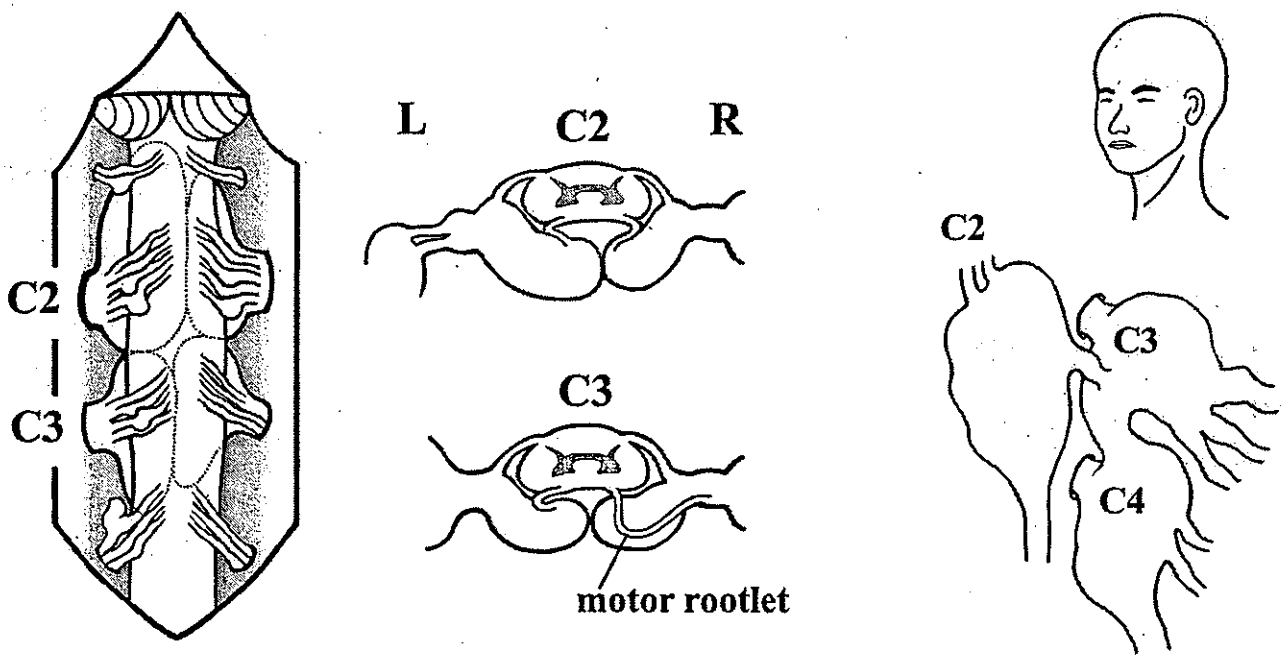

3 Intraoperative schematic drawing. **Left and middle:** Bilateral C2 and C3 root-related tumors were located ventrally to the spinal cord, showing a bilateral dumbbell pattern through the dura at the C1–2 level and C2–3 intervertebral foramina. The tumors involved both sensory and motor rootlets except for the right C3 root-related tumor, which involved the sensory rootlets alone. The motor rootlets associated with the tumors were elongated and tortuous (middle). **Right:** Tumors of the left neck: Note that the tumor stems from the C2 cervical nerve isolated from the C2 root-related dumbbell tumor. The tumor of C3 cervical nerve origin is continuous with the intradural mass through the C2-C3 intervertebral foramen. The tumor of C4 cervical nerve origin extends into the vertebral foramen, but there is no intradural mass as shown in the drawing on the left. None of the tumors was related to the cervical sympathetic nerve.

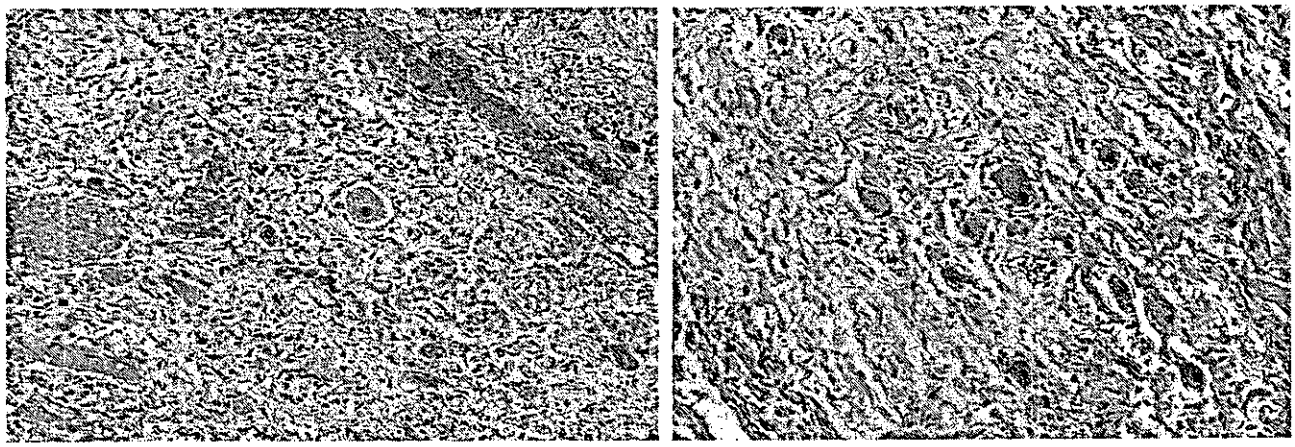

4 Pathologic findings of the tumors of the intradural space (left) and the cervical neck (right) showing mature ganglion cells and stroma containing spindle shaped cells. H&E, original magnification ×50.

intradural space and cervical neck was ganglioneuroma (Figure 4).

Discussion

Ganglioneuromas are a subgroup of peripheral neuroblastic tumors that have been defined as childhood embryonal tumors of migrating neuroectodermal cells derived from the neural crest [20,22]. Peripheral neuroblastic tumors are classified into three subgroups depending on the degree and type of neuroblastic differentiation and the degree of Schwannian stroma development: neuroblastomas, ganglioneuroblastomas and ganglioneuromas [22]. Immature neuroblastic tumors are reportedly capable of maturing into more differentiated forms, such as spontaneous or therapy-induced maturation of neuroblastoma or maturation from ganglioneuroblastoma to ganglioneuroma [2–4,7-10,24]. The final stage of maturation in the neuroblastic tumors is usually seen in patients more than 10 years old [22]. Ganglioneuromas, a mature form of neuroblastic tumors, are rare, slow-growing benign tumors characterized by a firm round or oval and well-encapsulated mass with occasional lobulations [2,22], occurring most frequently in children or young adults [2,9,10,15,19,21,25]. They can arise from the sympathetic nervous system extending from the skull base to the pelvis but mainly from the paraspinal sympathetic chain ganglia. Therefore, they are most commonly found in the posterior mediastinum and abdomen, where they usually arise from the adrenal medulla, and in the lumbar and pelvic retroperitoneal space [7,9,12,19,21,25]. A very few may originate from other locations or heterotopic areas, as well as from peripheral nerves (sensory ganglia or nerves) [9,11,16,25,27,28]. Multiple occurrences [19,21,23,27] and an association with von Recklinghausen's disease are another unusual feature [8,12,15,21,23,25]. Approximately 20 cases of ganglioneuromas associated with von Recklinghausen's disease have been reported [8,12,15,21,23,25], but the genetic association between von Recklinghausen's disease and ganglioneuromas is unclear. Ganglioneuromas of sympathetic chain origin usually develop as a paravertebral mass and may infrequently become dumbbell tumors extending into the spinal canal through one or more intervertebral foramina [21,27]. The term "dumbbell" is used to designate the growth pattern of the tumor such as in relation to the intervertebral foramen; intraspinal-extravertebral, intraspinal-foraminal, or foraminal-extravertebral; and also in relation to the dura in the spinal canal, intra-extradural [5,21,23]. The pattern may depend on whether the tumor originates from within or outside the spinal canal or within the intervertebral foramen. In many cases of dumbbell ganglioneuroma the intraspinal portion of the tumor extends extradurally [1–3,6,13–15,17,18,21,24–27], but intradural extension is extremely rare [21,23].

Ganglioneuromas of the cervical spine are also extremely rare, with only 5 pathologically confirmed and previously reported cases (Table 1) [13,21,23,26,27]. All these cases presented a dumbbell pattern. Intraspinal extradural expansion was seen in 3 patients [13,26,27], one of whom showed bilateral symmetric occurrence from both C2 nerve roots [27], while intradural expansion was observed in 2 patients, both of whom showed unilateral multiple occurrence as well as association with von Recklinghausen's disease [21,23]. It has been suggested that the origin of these tumors is related

to the sensory root ganglion or the intra- or extradural sensory root of the cervical nerve [21,23,26,27]. It is noteworthy that previously reported cervical intradural ganglioneuromas extended ventrally to the spinal cord, as seen in our case, even though they were suspected to have originated from the intradural sensory roots [21,23].

CONCLUSION

This report concerns an extremely rare case of ganglioneuromas in a 35-year-old man with von Recklinghausen's disease who presented bilateral and symmetric dumbbell ganglioneuromas with intradural extension. These tumors involved the bilateral C2 and C3 nerve roots and were also accompanied by multiple bilateral tumors at the neck. To the best of our knowledge, no such ganglioneuromas have been reported previously. In our case, the intradural tumors were suspected to have originated from the sensory ganglion and to have grown ventrally to the spinal cord, involving sensory as well as motor rootlets. The tumors could be removed without damage to the spinal cord because they did not adhere to the spinal cord. On the other hand, the isolated masses of the neck were suspected to have originated from the cervical nerve itself, perhaps from the sensory nerve, although the tumor of the C3 cervical nerve was continuous with the intradural C3 root-related mass through the vertebral foramen.

We consider this and previously reported cases to be of interest because they indicate that cervical spinal ganglioneuromas tend to originate from sensory roots or ganglia and to develop a dumbbell shape with occasional intradural extension followed by ventral growth to the spinal cord.

1 Summary of Reported Cervical Ganglioneuromas

Case No	Authors	Age & Sex	Dumbbell Pattern	Intraspinal Extension	Site	Multiplicity	Suspected Origin	vRHD	Others
1	Shephard, et al, 1958	35 y, M	1	intradural	right	+	intradural post root	+	located ventrally at C2-C7 levels
2	Sinclair, et al, 1961	44 y, F	2	intradural	right	+	intradural post root	+	located ventrally at C2-C5 levels
3	Suetake, et al, 1993	20 y, M	3	extradural	right	–	post root ganglion	NF2	C5 origin
4	Maggi, et al, 1995	18 m, F	3	extradural	left	–	neural crest remnant cell (intradural post root?)	–	located at C2-C6 levels
5	Ugarriza, et al, 2001	53 y, M	3	extradural	bilat	+	extradural post root	–	bilateral C2 origin, symmetric
6	Kyoshima, et al, 2002	35 y, M	4	intradural	bilat	+	post root ganglion	+	located ventrally, bilateral C2 and C3 origin, symmetric

vRHD, von Recklinghausen's disease; 1, intraspinal-foraminal (intradural-foraminal) pattern; 2, intra-extradural pattern; 3, intraspinal-extravertebral (extradural-extravertebral) pattern; 4, intraspinal-extravertebral (intradural-extravertebral) pattern; bilat, bilateral; post, posterior; NF2, neurofibromatosis type 2.

REFERENCES

1. Bauer BL, Bauer H, Griss P, et al. Dumb-bell ganglioneuroma of the spine misinterpreted as progressive idiopathic scoliosis. Case report. Arch Orthop Trauma Surg 1989;108:189–94.
2. Carpenter WB, Kernohan JW. Retroperitoneal ganglioneuromas and neurofibromas: a clinicopathological study. Cancer 1963;16:788–97.
3. Cote P, Cassidy JD, Dzus A, Yong-Hing K. Ganglioneuroma of the thoracic spine presenting as adolescent idiopathic scoliosis: a case report. J Spinal Disord 1994;7:528–32.
4. Dyke PC, Mulkey DA. Maturation of ganglioneuroblastoma to ganglioneuroma. Cancer 1967;20:1343–9.
5. Eden K. The dumb-bell tumours of the spine. Br J Surg 1941;28:549–70.
6. Fagan CJ, Swischuk LE. Dumbbell neuroblastoma or

ganglioneuroma of the spinal canal. AJR 1974;120: 453–60.
7. Geoerger B, Hero B, Harms D, Grebe J, Scheidhauer K, Berthold F. Metabolic activity and clinical features of primary ganglioneuromas. Cancer 2001;91:1905–13.
8. Geraci AP, de Csepel J, Shlasko E, Wallace SA. Ganglioneuroblastoma and ganglioneuroma in association with neurofibromatosis type I: report of three cases. J Child Neurol 1998;13:356–8.
9. Hamilton JP, Koop CE. Ganglioneuromas in children. Surg Gynecol Obstet 1965;121:803–12.
10. Hayes FA, Green AA, Rao BN. Clinical manifestations of ganglioneuroma. Cancer 1989;63:1211–4.
11. Levy DI, Bucci MN, Weatherbee L, Chandler WF. Intradural extramedullary ganglioneuroma: case report and review of the literature. Surg Neurol 1992;37: 216–8.
12. Lockhart ME, Smith JK, Canon CL, Morgan DE, Heslin MJ. Appendiceal ganglioneuromas and pheochromocytoma in neurofibromatosis type 1. AJR Am J Roentgenol 2000;175:132–4.
13. Maggi G, Dorato P, Trischitta V, Varone A, Civetta F. Cervical dumbbell ganglioneuroma in an eighteen month old child. A case report. J Neurosurg Sci 1995; 39:257–60.
14. Miura Y, Okumichi T, Yoshioka K, Okumichi K, Kajihara H. Successful excision of a "dumb-bell" shaped ganglioneuroma of the posterior mediastinum with a large intraspinal component. Eur J Surg 1993;159: 635–8.
15. Mutluer S, Ersahin Y, Binatli O, Demirtas E. Dumbbell ganglioneuromas in childhood. Childs Nerv Syst 1993; 9:182–4.
16. Ng TH, Fung CF, Goh W, Wong VC. Ganglioneuroma of the spinal cord. Surg Neurol 1991;35:147–51.
17. Oro JJ, Geise AW. Dumbbell ganglioneuroma of the lumbar spine associated with a herniated intervertebral disc: case report. Neurosurgery 1983;13:711–4.
18. Pascaud JL, Le Goff JJ, Pascaud E, Rousseau J. Thoracic ganglioneuroma with intra-spinal prolongations in childhood. Pediatr Radiol 1980;9:109–10.
19. Richardson RR, Reyes M, Sanchez RA, Torres H, Vela S. Ganglioneuroma of the sacrum. A case report. Spine 1986;11:87–9.
20. Schwab M, Schimada H, Brodeur GM. Neuroblastic tumors of adrenal gland and sympathetic nervous system. In: Kleihues P, Cavenee WK, eds. World Health Organization Classification of Tumours. Lyon: IARC Press, 2000:153–61.
21. Shephard RH, Sutton D. Dumbbell ganglioneuromata of the spine with a report of four cases. Br J Surg 1958;45:305–17.
22. Shimada H, Brodeur GM. Tumors of peripheral neuroblasts and ganglion cells. In: Bigner DD, McLendon RE, Bruner JM, eds. Russel and Rubinstein's Pathology of Tumors of the Nervous System, Volume 2, 6th ed. London: Arnold, 1998:493–533.
23. Sinclair JE, Yang YH. Ganglioneuroma of the spine associated with von Recklinghausen's disease. J Neurosurg 1961;18:115–9.
24. Skaggs DL, Roberts JM, Codsi MJ, Meyer BC, Moral LA, Masso PD. Mild gait abnormality and leg discomfort in a child secondary to extradural ganglioneuroma. Am J Orthop 2000;29:111–4.
25. Stout AP. Ganglioneuroma of the sympathetic nervous system. Surg Gynecol Obstet 1947;34:101–10.
26. Suetake K, Niwa J, Okuyama T, Hirai H, Shimoyama N, Ishidate T. [Ganglioneuroma in the cervical ganglion with neurofibromatosis-2: a case report]. No Shinkei Geka 1993;21:629–32.
27. Ugarriza LF, Cabezudo JM, Ramirez JM, Lorenzana LM, Porras LF. Bilateral and symmetric C1-C2 dumbbell ganglioneuromas producing severe spinal cord compression. Surg Neurol 2001;55:228–31.
28. Wilber MC, Woodcock JA. Ganglioneuroma in bone. J Bone Joint Surg 1957;39-A:1385–88.

COMMENTARY

The authors report an exceptional location of ganglioneuroma, which is a tumor arising from the paraspinal sympathetic chain, mostly in thoracolumbar area in children and young adults. The originality of this paper is the age of the patient (35 years old), the location of the tumor (cervical; only 5 cases previously described), the association with von Recklinghausen's disease (around 20 reported cases), and the nice way the authors solved the problem in two surgical steps: first by removing the intradural portion, second by removing the extravertebral tumor. Conversely to neuroblastomas and ganglioneuroblastomas, ganglioneuromas are the mature form of the two previous ones, thus being benign and surgically treatable. They may be completely removed and cured with staged intraspinal and extraspinal approaches, which was nicely done by the authors.

Jacques Brotchi, M.D., Ph.D.
Department of Neurosurgery
Erasme Hospital Univ. Brussels
Brussels, Belgium

Pulmonary Lymphoepithelioma-like Carcinoma: Predominant Infiltration of Tumor-associated Cytotoxic T Lymphocytes Might Represent the Enhanced Tumor Immunity

Motohiro KOBAYASHI, Makoto ITO, Kenji SANO, Takayuki HONDA and Jun NAKAYAMA

Reprinted from Internal Medicine
Vol. 43, No. 4, Pages 323–326
April 2004

□ CASE REPORT □

Pulmonary Lymphoepithelioma-like Carcinoma: Predominant Infiltration of Tumor-associated Cytotoxic T Lymphocytes Might Represent the Enhanced Tumor Immunity

Motohiro KOBAYASHI, Makoto ITO*, Kenji SANO**, Takayuki HONDA** and Jun NAKAYAMA

Abstract

Lymphoepithelioma-like carcinoma (LELC) of the lung is an undifferentiated carcinoma with prominent lymphoid stroma. We encountered a case of synchronous primary lung cancers of LELC and papillary adenocarcinoma in a 67-year-old Japanese woman. By in situ hybridization, Epstein-Barr virus (EBV) genome was detected in malignant epithelial cells of LELC but not in the papillary adenocarcinoma. Tumor-infiltrating lymphocytes in LELC were predominantly $CD8^+$ and T cell intracytoplasmic antigen (TIA-1)$^+$ cytotoxic T cells with closely associated with HLA-DR-positive LELC cells by double immunostaining. These data indicate that the exaggerated lymphoid infiltration in and around the EBV-infected carcinoma cells may represent the enhanced tumor immunity, suggesting a better prognostic indicator.

(Internal Medicine 43: 323–326, 2004)

Key words: lung cancer, lymphoepithelioma-like carcinoma, Epstein-Barr virus, HLA-DR, cytotoxic T cell

Introduction

Pulmonary lymphoepithelioma-like carcinoma (LELC), first described by Begin et al in 1987 (1), has been recognized as a rare but distinctive histologic variant among undifferentiated carcinomas (2–6), histologically identical to lymphoepithelial carcinomas arising in the nasopharynx and in other anatomic sites (7–10). Of particular interest is the close association between Epstein-Barr virus (EBV) infection and the occurrence of pulmonary LELC in Asian and related ethnic populations (5). Here, we report a case of synchronous primary lung cancer presenting with LELC and papillary adenocarcinoma involving different lobes. The association of EBV infection with these tumors is examined by in situ hybridization. Immunohistochemical profile of the tumor infiltrating lymphocytes in LELC is also precisely evaluated.

Case Report

A 67-year-old Japanese woman was admitted to the hospital to have an operation for osteoarthrosis of bilateral knee joints. Although she was entirely asymptomatic, systemic preoperative evaluation revealed a circumscribed mass lesion, 4 cm in diameter, in the region of the right middle lobe of the lung on chest roentgenogram (Fig. 1A). In addition, computed tomography disclosed another smaller coin lesion, that was initially considered as a metastatic lesion, in the periphery of the right lower lobe (Fig. 1B). Sputum cytology and bronchoscopic biopsy, however, failed to demonstrate malignant cells. After 131 days from the first admission, she undertook exploratory thoracotomy. Intraoperative frozen section of the right hilar lymph node disclosed a metastatic non-small cell carcinoma. Consequently, even though a stage IIIA lung cancer was suspected, a combined right middle and lower lobectomy with a regional lymph node dissection were performed. Her postoperative course was uneventful. After discharge, she received an adjuvant irradiation, and the patient remained free from any signs of tumor progression for over 5 years.

From Department of Pathology, **Laboratory Medicine, Shinshu University School of Medicine, Matsumoto and *Division of Diagnostic Pathology, Department of Pathology and Laboratory Medicine, Kariya General Hospital, Kariya

Received for publication July 31, 2003; Accepted for publication November 5, 2003

Reprint requests should be addressed to Dr. Motohiro Kobayashi, Department of Pathology, Shinshu University School of Medicine, 3-1-1 Asahi, Matsumoto 390-8621

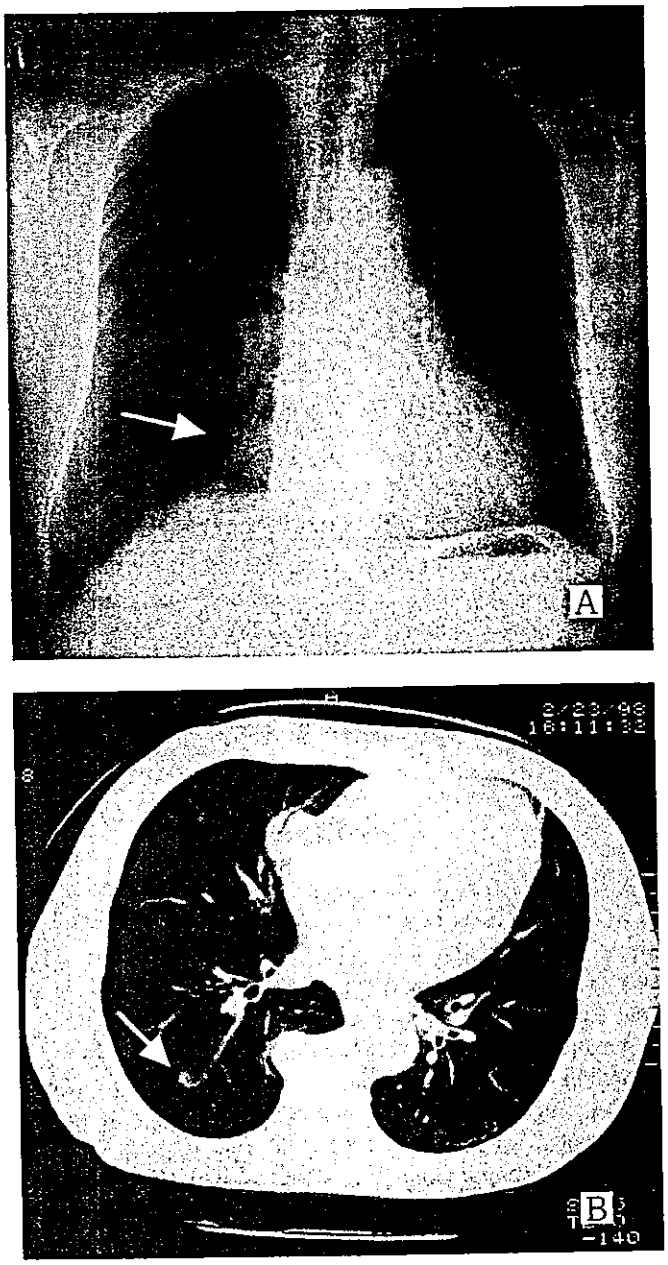

Figure 1. Radiologic features of this case. (A) Chest roentgenogram reveals a large mass lesion adjacent to the pericardium (arrow). (B) Chest CT reveals another small coin lesion in the periphery of the right lower lobe (arrow).

Pathological Findings

Gross examination of the specimen demonstrated a well-circumscribed solid tumor, 2 by 3 cm in maximal dimension, in the right middle lobe, and a small nodular tumor, 7 mm in diameter, in the subpleural region of the right lower lobe. Several hilar lymph nodes were swollen. Histologically, the tumor of the right middle lobe showed the characteristic histological appearance consistent with lymphoepithelial carcinoma. The tumor cells showed a syncytial trabecular growth of undifferentiated epithelial cells separated by abundant lymphoid stroma (Fig. 2A). The tumor cells were oval in shape with paler cytoplasm, vesicular nucleus, and one or two prominent nucleoli (Fig. 2B). The metastatic lesion of the lymph node also showed the same histology. In the lymphoid stroma there were scattered caseation-like tumor necrotic foci with dystrophic calcification accompanied by multinucleated giant cell reaction. On the other hand, the tumor of the right lower lobe was a well-differentiated papillary adenocarcinoma with fibrous stroma and sparse lymphocytic infiltrates.

Immunohistochemical study showed that the LELC cells were strongly positive for cytokeratin CAM 5.2 (Fig. 2C) and HLA-DR antigens (Fig. 2D). In the lymphoid stroma, there were more frequent CD45RO-positive T cells (Fig. 2E) than CD20-positive B cells (Fig. 2F). The latter cells collectively formed lymphoid follicles with a germinal center. Among the T-cell population, there were more $CD8^+$ cells than $CD4^+$ cells. The lymphocytes infiltrating into the tumor cell nests were almost exclusively positive for CD8 (Fig. 2D) and T cell intracytoplasmic antigen (TIA-1) (Fig. 2G). Both LELC and papillary adenocarcinoma were negative for latent membrane protein 1 (LMP1) (data not shown). Ki-67 (MIB-1) labeling index was 12.3% in malignant epithelial cells as compared to 5.9% in surrounding lymphoid stroma. The labeling index of metastatic carcinoma cells in lymph nodes was 34.9%.

In situ hybridization for EBV genome showed positive signals confined to malignant epithelial cells of the LELC (Fig. 2H). In contrast, no signals were detected in the papillary adenocarcinoma (data not shown).

Discussion

Primary LELC of the lung, which is histologically analogous to those occurring elsewhere, refers to a specialized variant of undifferentiated carcinomas with prominent lymphoid stroma (1, 2). Ultrastructurally, the tumor cells retain cytological features reminiscent of squamous cell differentiation (2). As far as we know, 28 cases of pulmonary LELC, including the present case, have been described in the literature, among which 20 cases occurred in Asian and related ethnic patients (1–6). It is intriguing that the strong association of EBV infection with pulmonary LELC has been demonstrated only in Asian patients and not in Caucasian patients (6). In the present case, the EBV genome was identified in the LELC cells alone, while not in papillary adenocarcinoma. This fact may relate to its viral tropism toward the complement receptor CR2 (CD21) present on nasopharyngeal epithelial cells, B lymphocytes, and follicular dendritic cells. An EBV endemicity in Asian countries is in all likelihood related to the overall higher incidence of EBV-associated lymphoepithelial neoplasms in a variety of organs, including nasopharynx (7), stomach (8), thymus (9),

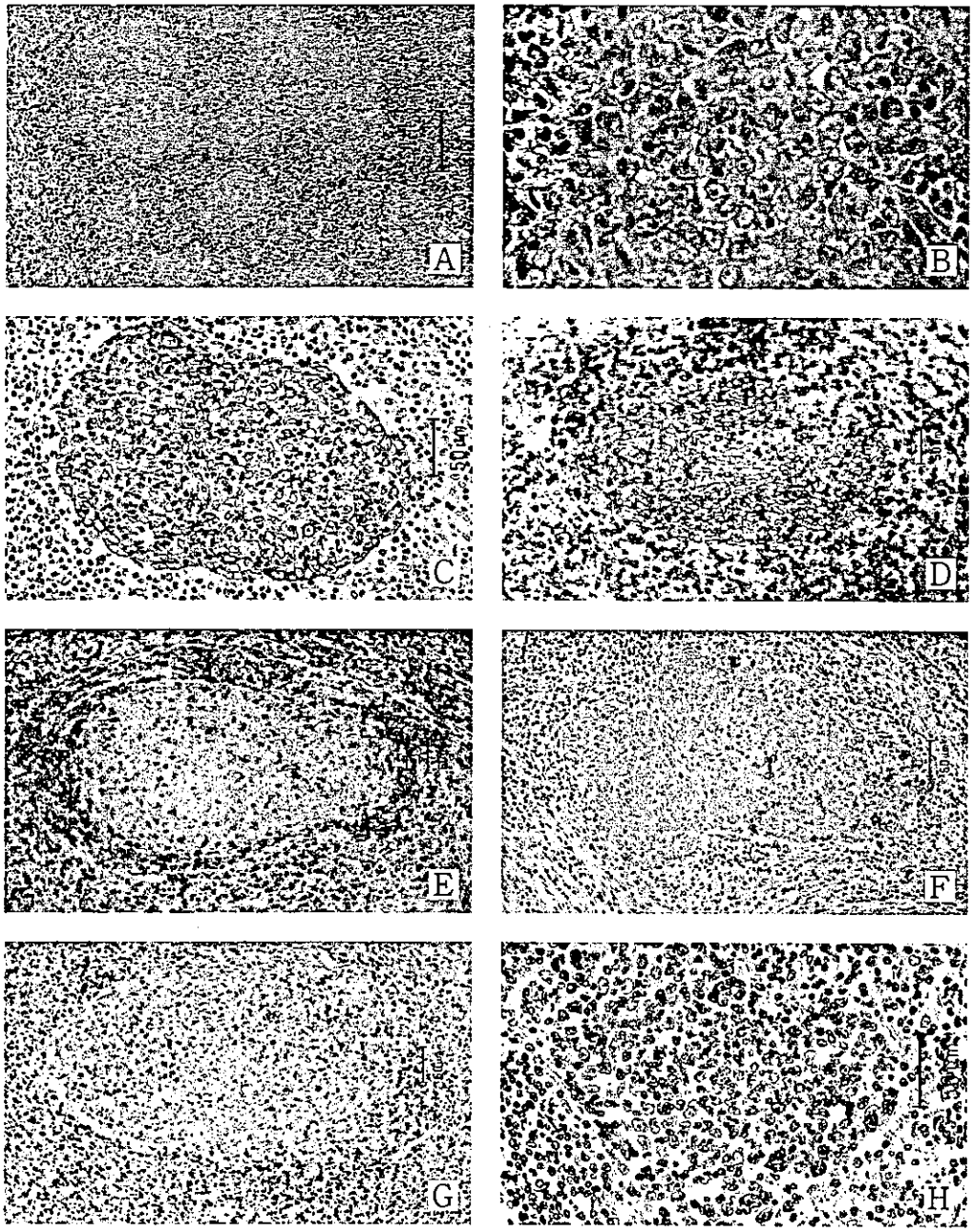

Figure 2. Histopathology of the surgical specimen. (A) Undifferentiated epithelial tumor cells of the middle lobe grow in a cord and nest pattern surrounded by lympho-plasmacytic cells. A substantial number of lymphocytes also infiltrate into the tumor cell nest (HE stain, ×100). (B) The epithelial tumor cells are oval in shape with paler cytoplasm, vesicular nucleus, and one or two prominent nucleoli (HE stain, ×800). (C) Lymphoepithelioma-like carcinoma (LELC) epithelial cells are strongly immunopositive for cytokeratin CAM 5.2 (×400). (D) Double immunohistochemical staining. The paraffin section was pretreated with microwave-irradiated antigen retrieval for 30 minutes in 1 mM EDTA-3Na solution (pH 8.0). To detect HLA-DRβ, anti-human HLA-DRβ mouse monoclonal antibody (DAKO, Kyoto) was used. The LELC cell membrane is selectively immunopositive for HLA-DRβ (brown), and the lymphocytes in and around the carcinoma cell nest are predominantly CD8 positive cells (red). Brown coloration represents oxidized DAB reaction products catalyzed by horseradish peroxidase, while red coloration is produced by Vector™ Red Alkaline Phosphatase Substrate Kit I (Burlingame, CA) (×200). (E) Immunostaining for CD45RO (×200). (F) Immunostaining for CD20 (×200). Most of the lymphocytes in and around the epithelial tumor cells are T cells. (G) Immunoperoxidase staining by T cell intracytoplasmic antigen (TIA-1). $CD8^+$ lymphocytes infiltrating into and around tumor cell nest in Fig. 1D are also positive for TIA-1 (×200). (H) In situ hybridization for Epstein-Barr virus (EBV) genome with FITC-labeled EBV oligo DNA probe (DAKO, Kyoto) using paraffin section. Hybridized signals were detected with anti-FITC antibody conjugated to alkaline phosphatase. New Fuchsin was used as the chromogen. Hybridized signals are confined to nuclei of LELC cells (red) (×400).

and salivary gland (10). It is said that EBV-infected cells express LMP1 that is a viral analogue of the family of tumor necrosis factor receptors in human cells, and that mediates the transforming role of EBV in B lymphocytes (11). In the present case, however, immunohistochemical study demonstrated that neither epithelial cells nor stromal lymphocytes of LELC express LMP1. It is said that LMP1 is frequently expressed in nasopharyngeal lymphoepithelioma and in lymphomas, but it has been shown that no carcinoma in other sites expressed such viral protein (12). Furthermore, in some LELC patients, especially in Caucasian patients, no EBV genome was detected. Hence, it can be postulated that certain genetic predisposition and environmental factors of as yet to be defined significance may account for the tumorigenesis of different types of EBV-associated carcinomas in different geographical areas.

It is of little doubt that persistent EBV infection is related to the occurrence of exaggerated lymphoid cell proliferation in lymphoepithelial neoplasms. Thomas and coworkers (7) demonstrated that T-helper/inducer ($CD4^+$) and T-suppressor/cytotoxic ($CD8^+$) cells constitute the majority of infiltrating lymphocytes in nasopharyngeal lymphoepithelial carcinoma. Furthermore, Saiki et al (13) demonstrated that in EBV-associated lymphoepithelial carcinoma of the stomach, the infiltrating lymphocytes within the tumor cell nests are actively proliferative $CD8^+$ lymphocytes expressing perforin. They concluded that such immunophenotypic features of the tumor-infiltrating lymphocytes, together with the enhanced HLA-DR expression in malignant epithelial cells, correlate with the overall better prognosis of the EBV-associated gastric cancers. In the present case, the tumor-infiltrating lymphocytes exhibited the same immunohistochemical profile, which suggests that the preponderance of $CD8^+$ lymphocytes over $CD4^+$ lymphocytes can be linked to their enhanced tumoricidal activity against EBV-infected malignant cells. Tumor-infiltrating lymphocytes might behave as tumor-suppressing immune effector cells to minimize the invasion of neoplasm. Apart from these assumptions, there is limited information currently available on the prognosis of pulmonary LELC (6). The present case suggests that the higher proliferative index of tumor cells does not necessarily warrant a favorable prognostic outlook. However, only one recurrent case has been recorded in the patients with stages I and II pulmonary LELC (6).

Acknowledgements: We would like to express thanks to Professor Emeritus Masao Hotchi and Professor Tsutomu Katsuyama for their helpful suggestions throughout this study. We also express appreciation to Ms. Yasuyo Shimojo, Akiko Ishida, and Kyoko Sakura for their technical assistance.

References

1) Begin LR, Eskandari J, Joncas J, Panasci L. Epstein-Barr virus related lymphoepithelioma-like carcinoma of lung. J Surg Oncol **36**: 280–283, 1987.
2) Butler AE, Colby TV, Weiss L, Lombard C. Lymphoepithelioma-like carcinoma of the lung. Am J Surg Pathol **13**: 632–639, 1989.
3) Pittaluga S, Wong MP, Chung LP, Loke SL. Clonal Epstein-Barr virus in lymphoepithelioma-like carcinoma of the lung. Am J Surg Pathol **17**: 678–682, 1993.
4) Higashiyama M, Doi O, Kodama K, et al. Lymphoepithelioma-like carcinoma of the lung: analysis of two cases for Epstein-Barr virus infection. Hum Pathol **26**: 1278–1282, 1995.
5) Wockel W, Hofler G, Popper HH, Morresi A. Lymphoepithelioma-like carcinoma of the lung. Pathol Res Pract **191**: 1170–1174, 1995.
6) Frank MW, Shields TW, Joob AW, et al. Lymphoepithelioma-like carcinoma of the lung. Ann Thorac Surg **64**: 1162–1164, 1997.
7) Thomas JA, Iliescu V, Crawford DH, Ellouz R, Cammoun M, de-The G. Expression of HLA-DR antigens in nasopharyngeal carcinoma: an immunohistochemical analysis of the tumor cells and infiltrating lymphocytes. Int J Cancer **33**: 813–819, 1984.
8) Burke AP, Yen TS, Shekitka KM, Sobin LH. Lymphoepithelial carcinoma of the stomach with Epstein-Barr virus demonstrated by polymerase chain reaction. Mod Pathol **3**: 377–380, 1990.
9) Dimery IW, Lee JS, Blick M, Pearson G, Sptizer G, Hong WK. Association of the Epstein-Barr virus with lymphoepithelioma of the thymus. Cancer **61**: 2475–2480, 1988.
10) Hamilton-Dutoit SJ, Therkildsen MH, Nielsen NH, Jensen H, Hansen JP, Pallesen G. Undifferentiated carcinoma of the salivary gland in Greenlandic Eskimos: demonstration of Epstein-Barr virus DNA by in situ nucleic acid hybridization. Hum Pathol **22**: 811–815, 1991.
11) Liebowitz D. Epstein-Barr virus and a cellular signaling pathway in lymphomas from immunosuppressed patients. N Engl J Med **338**: 1413–1421, 1998.
12) Chang YL, Wu CT, Shih JY, Lee YC. New aspects in clinicopathologic and oncogene studies of 23 pulmonary lymphoepithelioma-like carcinomas. Am J Surg Pathol **26**: 715–723, 2002.
13) Saiki Y, Ohtani H, Naito Y, Miyazawa M, Nagura H. Immunophenotypic characterization of Epstein-Barr virus-associated gastric carcinoma: massive infiltration by proliferating $CD8^+$ T-lymphocytes. Lab Invest **75**: 67–76, 1996.

The Japanese Society of Internal Medicine
28-8, 3-chome, Hongo, Bunkyo-ku, Tokyo 113-8433, Japan

AJNR Am J Neuroradiol 25:766–768, May 2004

Case Report

Degenerative Thalamic Hamartoma: CT and MR Imaging Features

Tomoki Kaneko, Rei Kawakami, Yasunari Fujinaga, Kazuhiro Oguchi, Jun Nakayama, Kazuhiro Hongo, and Masumi Kadoya

Summary: We describe hamartomas of possible thalamic origin. CT revealed marked calcification in the mass lesion, and MR imaging revealed contrast enhancement. Histologically, outgrowth of the glia was observed, but no neoplastic component was confirmed. Immunohistochemical staining was positive for the cell-adhesion factor N-CAM and negative for polysialic acid.

Neuronal hamartomas typically arise from the region of the hypothalamus and often present with precocious puberty, mass effect, or gelastic seizures. In this report, we describe the characteristics of a patient with a neuronal hamartoma that we hypothesize originated from the thalamus owing to embryologic and histopathologic characteristics and discuss the pathogenetic process of hamartomas, referring to previous reports.

Case Report

An 8-year-old boy had a history of left arm shaking and a decrease of grip strength for 6 months before presenting to our hospital. Abnormal hearing in his left ear had been observed 2 years earlier but had temporarily improved. Audiometry performed 2 months before admission, however, revealed decreased hearing in his left ear. His medical history was complicated by a ventricular septal defect (VSD) observed immediately after his birth, for which he has been receiving periodic treatment. He had no cognitive deficits and had been noted to develop normally.

Radiologic Findings

Noncontrast CT (Fig 1) performed to evaluate the patient's hearing loss revealed a hypoattenuated mass lesion relative to gray matter in the right thalamus. Marked calcifications were noted in the center of the mass lesion. MR imaging (Figs 2 and 3) of the mass demonstrated low signal intensity on T1-weighted images and high signal intensity on T2-weighted images relative to gray matter. The region with calcium enhanced on postcontrast T1-weighted MR images, but surrounding regions did not appear to enhance. The center of the lesion demonstrated signal intensity characteristics similar to those of CSF. The mass lesion protruded into the third ventricle and was surrounded by normal-appearing brain parenchymal tissue in a beaklike fashion. The internal capsule and remaining thalamus were compressed by the mass lesion. There was no evidence of extension of the mass into the hypothalamic region. The mass significantly compressed the tectum mesencephali, which was the likely cause for the patient's hydrocephalus.

Surgery and Pathology

On the basis of imaging findings, a glioma arising from the thalamus was suspected and craniotomy was performed. Intraoperative frozen sections did not reveal a neoplastic component, so a more extensive biopsy of the calcified region was performed. Histopathologic study of these biopsies confirmed the presence of a typical neuronal hamartoma.

Histopathologic study revealed a proliferation of vessels as well as minute calcifications. Gliosis owing to proliferation of astrocytes was observed, but there were no atypical cells or mitotic nucleus. Immunohistochemical staining was positive for the cell-adhesion factor N-CAM and negative for polysialic acid (Fig 4). MR imaging performed 6 months after the operation revealed no increase in the size of the mass lesion.

Discussion

Neuronal hamartoma is a rare entity arising from the hypothalamus region and typically projects into the interpeduncular fossa, between the pituitary infundibulum and the mamillary bodies (1). Patients, often younger than 3 years, tend to present with early onset of precocious puberty. Male sex predominance has been noted (2, 3). Hypothalamic hamartomas are regarded as a heterotopia and are composed of well-differentiated neuroglial tissue (1, 2). On MR images, the lesions are isointense to gray matter and do not typically demonstrate contrast enhancement on T1-weighted images. They are typically hyperintense on T2-weighted images (1, 2). Cyst formations and calcifications have been rarely reported (1, 2, 4).

In our case, two atypical imaging findings were demonstrated: the hamartoma originated in the thalamus, and contrast enhancement was observed in the area of the calcified portion. Hamartomas, though most often associated with the hypothalamus, have been reported as arising in the thalamus (5), as in our case. Embryologically, the thalamus and hypothalamus are differentiated from the diencephalon, which develops in the 5th gestational week, and are anatomically separated by the hypothalamic sulcus in the 7th gestational week (6). Therefore, in our case, hamartoma was thought to occur in the diencephalon before the thalamus and hypothalamus were differentiated. Because the thalamus and hypothalamus could have

Received October 1, 2002; accepted after revision September 16, 2003.

From the Departments of Radiology (T.K., R.K., Y.F., M.K.), Pathology (K.O.), and Neurosurgery (J.N., K.H.), Shinshu University School of Medicine, Matsumoto, Japan.

Address correspondence to Tomoki Kaneko, MD, Department of Radiology, Shinshu University School of Medicine, 3-1-1 Asahi, Matsumoto 390-8621 Japan.

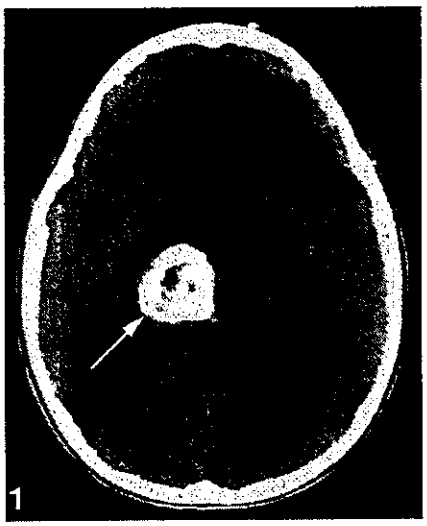

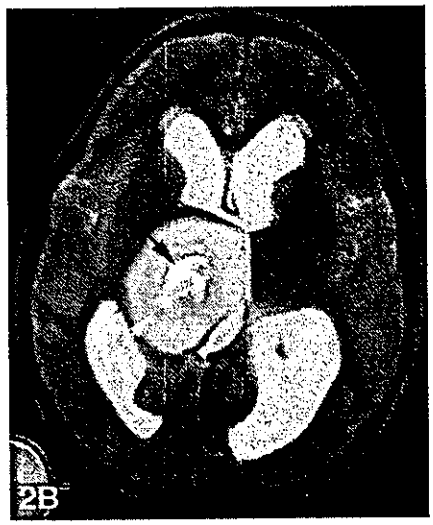

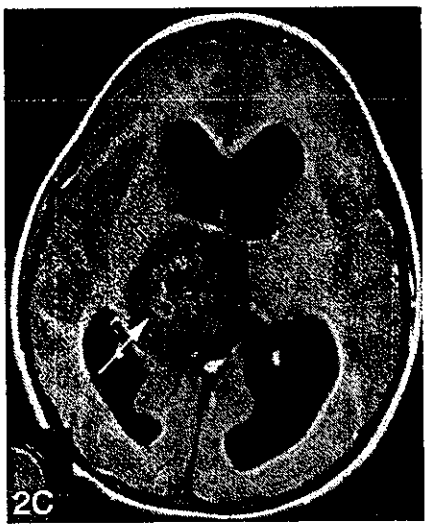

FIG 1. Noncontrast CT scan shows a low-attenuation mass in the right thalamus. Marked calcifications are seen in the center of the mass lesion (*arrow*).

FIG 2. Axial MR images. All images are obtained at same level.
A, T1-weighted image (500/20 [TR/TE]). *B*, T2-weighted image (5000/88 [TR/TE]). *C*, T1-weighted (500/20 [TR/TE]) image after gadolinium-DTPA administration.
The mass lesion shows lower signal intensity on the T1-weighted image (*A*) and higher signal intensity on the T2-weighted MR image (*B*) relative to gray matter. Calcified regions show slightly greater signal intensity on the T1-weighted image (*A*) and are enhanced after administration of gadolinium-DTPA (*C*, *light arrows*). CSF-like signal intensity exists in the core of the lesion (*dark arrows*).

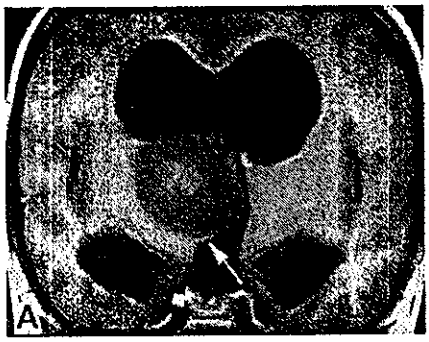

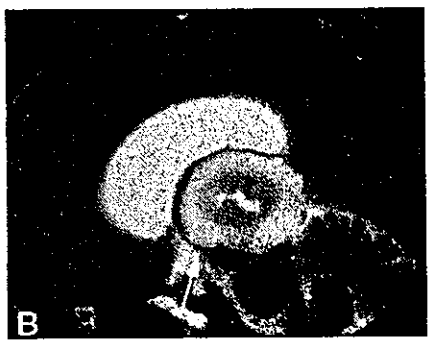

FIG 3. *A*, Coronal image after administration of gadolinium-DTPA (500/20 [TR/TE]). *B*, Sagittal T2-weighted image (4000/88.9 [TR/TE]). The margin of the mass lesion is covered with thalamus extending in a beaklike shape (*arrows*).

migrated owing to the hamartoma in the diencephalon, our case could be explained as an embryonic phenomenon. Sasaki et al reported on a hamartoma occurring in the lateral ventricle (7). In their case, it was possible that hamartoma developed in the roof plate of the diencephalon because of migration into the lateral ventricle.

Hypothalamic hamartoma is the primary feature of Pallister-Hall syndrome. Other major manifestations of the syndrome include polydactyly, imperforate anus, and hypopituitarism (8). Reported congenital heart defects include patent ductus arteriosus and VSD (9). Our case was complicated with VSD. The membranous part of the interventricular septum is formed during the 6th–7th gestational week (10). Therefore, if hamartoma occurred in the diencephalons, as we suspect, this defect of the interventricular septum may have developed at almost the same time as the hamartoma, and our patient had one of subtypes of Pallister-Hall syndrome.

Because cystic change, calcification, and contrast enhancement at MR imaging can be observed in hamartoma, Prasad et al (4) reported that cystic changes in hamartoma are caused by hemorrhage or

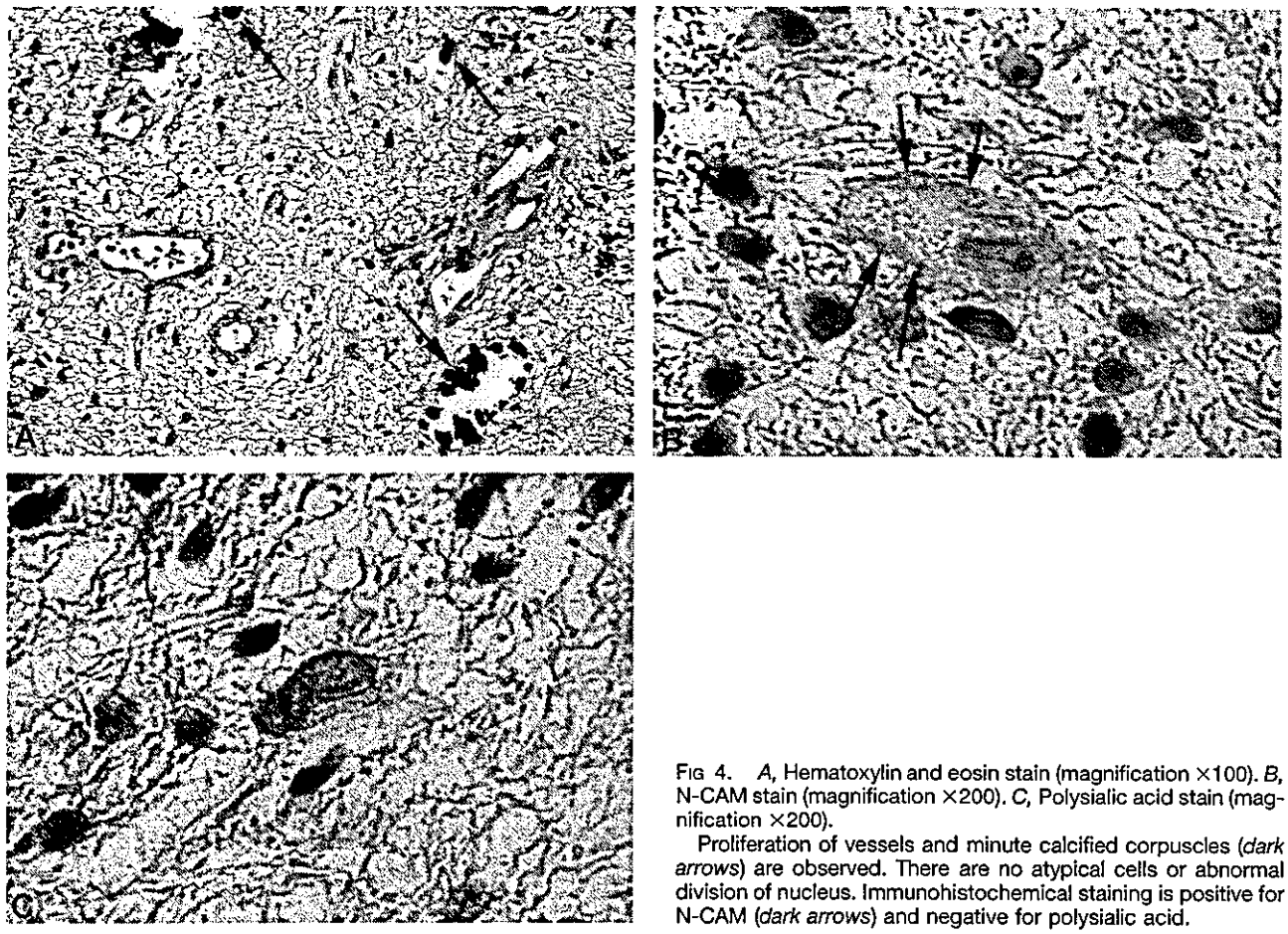

FIG 4. *A*, Hematoxylin and eosin stain (magnification ×100). *B*, N-CAM stain (magnification ×200). *C*, Polysialic acid stain (magnification ×200).

Proliferation of vessels and minute calcified corpuscles (*dark arrows*) are observed. There are no atypical cells or abnormal division of nucleus. Immunohistochemical staining is positive for N-CAM (*dark arrows*) and negative for polysialic acid.

liquefactive necrosis resulting from ischemic change in it. In addition, they thought that cystic changes seen in their case might be attributed to ischemic necrosis, in view of the size of the lesions. It was thought that ischemic change due to the increase of hamartoma caused hemorrhage and then degeneration, and calcifications occurred in our case. In addition, enhancement in hamartoma after administration of contrast medium was thought to be caused by vascular hyperplasia.

Although our patient had the mass lesion that was large enough to cause hydrocephalus, he had only symptoms related to compression of the corticospinal tract. When hamartoma occurs in the regions that do not cause severe disorders, including hypothalamic disorders, no symptoms might be observed in some cases.

Immunohistochemical staining was positive for N-CAM and negative for polysialic acid. N-CAM is a cell-adhesion factor, and polysialic acid exists in N-CAM and prevents cell adhesion. Polysialic acid is present in ganglion migration in the embryonic brain and, with some exceptions, is not observed in the adult brain (11). Polysialic acid was negative in our case, which strongly suggested that the hamartoma was composed of the differentiated tissues. Thus, our results positively supported the principle of performing follow-up observations for patients confirmed to have hamartoma.

References

1. Osborn AG. *Diagnostic Neuroradiology.* St. Louis, Mo: Mosby; 1994;481
2. Orrison WW Jr. *Neuroimaging.* Philadelphia: WB Saunders; 1998; 1594–1596
3. Barkovich AJ. *Pediatric Neuroimaging.* 3rd ed. Philadelphia: Lippincott-Raven; 1995;518–519
4. Prasad S, Shah J, Patkar D, Gala B, Patankar T. **Giant hypothalamic hamartoma with cystic change: report of two cases and review of the literature.** *Neuroradiology* 2000;42:648–650
5. Rossiter JP, Khalifa MM, Nag S. **Diencephalic neuronal hamartoma associated with congenital obstructive hydrocephalus, anophthalmia, cleft lip and palate and severe mental retardation: a possible new syndrome.** *Acta Neuropathol* 2000;99:685–690
6. Sadler TW. *Langman's Medical Embryology.* 8th ed. Philadelphia: Lippincott-Raven; 2000;432–433
7. Sasaki T, Matsuno A, Inoh Y, Asai A, Kirino T. **A rare case of hamartoma in the lateral ventricle: case report.** *Surg Neurol* 1997; 47:23–27
8. Gorlin RJ, Cohen MM, Jr, Levin LS. *Syndromes of the Head and Neck.* 3rd ed. New York: Oxford University Press; 1990;903–905
9. Biesecker LG, Graham JM Jr. **Pallister-Hall syndrome.** *J Med Genet* 1996;33:585–589
10. Sadler TW. *Langman's Medical Embryology.* 8th ed. Philadelphia: Lippincott-Raven; 2000;230–232
11. Nakayama J, Angata K, Ong E, et al. **Polysialic acid, a unique glycan that is developmentally regulated by two polysialyltransferases, PST and STX, in the central nervous system: from biosynthesis to function.** *Pathol Int* 1998;48:665–677

[CANCER RESEARCH 64, 4257–4262, June 15, 2004]

Functional Correlation of Trophinin Expression with the Malignancy of Testicular Germ Cell Tumor

Shingo Hatakeyama,[1] Chikara Ohyama,[1] Shingo Minagawa,[1] Takamitsu Inoue,[1] Hideaki Kakinuma,[1] Atsushi Kyan,[2] Yoichi Arai,[2] Tomoaki Suga,[3] Jun Nakayama,[4] Tetsuro Kato,[1] Tomonori Habuchi,[1] and Michiko N. Fukuda[5]

[1]Department of Urology, Akita University School of Medicine, Akita, Japan; [2]Department of Urology, Tohoku University School of Medicine, Sendai, Japan; [3]Department of Internal Medicine, Shinshu University School of Medicine and [4]Department of Pathology, Shinshu University Graduate School of Medicine, Matsumoto, Japan; and [5]Glycobiology Program, Cancer Research Center, The Burnham Institute, La Jolla, California

ABSTRACT

Trophinin is a membrane protein that is potentially involved in human embryo implantation by mediating homophillic cell adhesion between trophoblastic cells and endometrial cells. Trophinin expression by maternal cells may be induced by the embryo that secretes human chorionic gonadotropin (hCG). Because the process of tumor metastasis resembles that of trophoblast invasion and proliferation during embryo implantation, we hypothesized that testicular cancers that synthesize hCG express trophinin thus becoming aggressive trophoblast-like cells. We screened paraffin-embedded orchiectomy specimens of 158 patients with testicular germ cell tumor by immunohistochemistry using antitrophinin antibody. This screening identified trophinin-positive specimens with the frequencies 39 of 91 (43%) in stage I, 14 of 24 (58%) in stage II, and 41 of 43 (95%) in stage III ($P < 0.001$). Thus, trophinin expression positively correlates with clinical stage. Remarkably, trophinin was found in all of the cases (33 of 33) with lung metastasis. The levels of serum hCG-β were significantly higher in the patients with trophinin-positive tumors than those with trophinin-negative tumors ($P = 0.004$). To determine whether trophinin promotes aggressiveness of the cell, trophinin-negative human seminona cell line JKT-1 was stably transfected with a mammalian expression vector containing trophinin cDNA. *In vitro* assays revealed that trophinin-expressing JKT-1-Tro cells are more invasive than JKT-1-mock cells, whereas there are no differences between JKT-1-Tro and JKT-1-mock in their proliferation activity. Upon orthotopic inoculation to athymic nude mice, JKT-1-Tro cells exhibited i.p. metastases in all of the mice ($n = 5$), whereas JKT-1-mock produced no metastases ($n = 5$). These results suggest strongly that trophinin enhances invasiveness of the cells and promotes metastasis of testicular germ cell tumor.

INTRODUCTION

Testicular germ cell tumor remains the most common solid malignancy in young men between 15 and 35 years of age (1). Recent statistics suggest disturbing trends that incidence of testicular germ cell tumor is increasing, and the age at which testicular germ cell tumor develops is becoming younger (2, 3). With the introduction of *cis*-platinum chemotherapy in the late 1970s, the survival rate of patients with testicular germ cell tumor now exceeds 90% (4, 5). However, it is still difficult to treat advanced testicular germ cell tumor with multiple distant metastases.

In germ cell tumors, all of the patients of choriocarcinoma, 40–60% of embryonal carcinoma, and 5–10% of patients with pure seminoma show the elevation of human chorionic gonadotrophin (hCG) β in their sera (6). The hCG is a 38-kDa glycoprotein, which is composed of α and β polypeptide chains. The hCG is normally produced by trophoblastic cells in the placenta (7). The β subunit of hCG is one of the tumor markers of germ cell tumors, and this value correlates well with the patient populations having clinical stages I, II, and III testicular tumors (6).

Trophinin is a membrane protein that potentially mediates the initial adhesion between human embryo and uterine epithelial cells through a unique apical cell adhesion between two cell types, trophoblastic cells and endometrial epithelial cells (8–10). In humans, endometrium is under strict hormonal control and is generally not permissive to implantation. Trophinin is not expressed during proliferative and ovulation phases, whereas strong expression of trophinin within a restricted area of human endometrium was detected at early secretory phase or time of implantation window (8–10). Recent findings of ectopic pregnancy suggest strongly that trophinin expression by maternal cells is embryo-dependent. Thus, hCG-β secreted from the implanting embryo induces trophinin in maternal cells through jaxtacrine manner (11).

The processes of human embryo implantation, which include rapid proliferation and invasion of trophoblasts, are often compared with the aggressive behaviors of malignant cancer cells (12). Recent studies have suggested that hCG expressed in trophoblast and various malignant tumors promotes cellular motility (6–7). These observations prompted us to investigate the possible role of hCG in testicular germ cell tumors. We describe here the expression of trophinin and hCG-β in testicular germ cell tumors and the effect of ectopic expression of trophinin on cellular motility, proliferation, and metastatic activities.

MATERIALS AND METHODS

Human Testicular Germ Cell Tumor Specimens. Testicular germ cell tumor specimens from 158 patients (76 seminoma and 82 nonseminomatous germ cell tumors) at various clinical stages were collected between 1981 and 2002. Informed consent was obtained from all of the patients whose specimens were used in this study. Pathological findings were recorded according to American Joint Committee on Cancer staging system (13).

Serum hCG-β Measurement. Before orchiectomy, blood sample was obtained by routine venipuncture from each patient and was subjected to serum hCG-β subunit measurement by ELISA.

Immunohistochemistry. Immunohistochemistry for trophinin, tastin, and bystin was performed as described previously (14), except Simple Stain Max PO kit and Simple Stain AEC solution (Nichirei Corp., Tokyo, Japan), according to manufacturer's instructions. Anti-hCG antibody was obtained from Nichirei Corporation.

Cell Line and Cell Culture. JKT-1 is a human testicular seminoma cell line provided by Dr. Keigo Kinugawa (Department of Urology, Kawasaki Medical School, Kurashiki, Japan; Ref. 15). This cell line was maintained in α-MEM containing 10% fetal bovine serum in a humidified 5% CO_2 atmosphere at 37°C.

Establishment of Stable Transfectant. JKT-1 cells, which do not express trophinin, were transfected with pcDNA1-trophinin (8) using LipofectAMINE (Life Technologies, Inc.) as described in the protocol provided by the supplier. After 2 weeks in G418 selection (400 μg/ml; Life Technologies, Inc.), 20 single colonies were examined for immunochemical detection of trophinin using antitrophinin mouse monoclonal antibody and FITC-conjugated goat affinity-purified $F(ab')_2$ fragment specific to mouse IgM (Cappel). Three stable transfectants expressing trophinin were established (JKT-1-Tro). Among

Received 3/1/04; revised 3/29/04; accepted 4/7/04.

Grant support: Grants 15659377 (to C. Ohyama) and B-15390115 (to J. Nakayama) from the Japan Society for the Promotion of Science, a grant from Kyowa Medex (to M. Fukuda), and NIH Grant HD34108 (to M. Fukuda).

The costs of publication of this article were defrayed in part by the payment of page charges. This article must therefore be hereby marked *advertisement* in accordance with 18 U.S.C. Section 1734 solely to indicate this fact.

Requests for reprints: Michiko N. Fukuda, Glycobiology Program, Cancer Research Center, The Burnham Institute, 10901 North Torrey Pines Road, La Jolla, CA 92037. Phone: (858) 646-3143; Fax: (858) 646-3193; E-mail: michiko@burnham.org.

Table 1 *Association of trophinin immunostaining and clinical stage*

Study group	All positive/ total (%)	Seminoma positive/ total (%)	NSGCT[a] positive/ total (%)
Clinical stage			
I + II	39 + 14/91 + 24 (46)	17 + 6/56 + 12 (34)	22 + 8/35 + 12 (64)
III	41/43 (95)	6/8 (75)	28/28 (100)
P	<0.001	<0.05	<0.001
Lung metastasis			
–	61/125 (49)	24/71 (34)	37/54 (69)
+	33/33 (100)	5/5 (100)	28/28 (100)
P	<0.001	<0.05	<0.001

[a] NSGCT, nonseminomatous germ cell tumor.

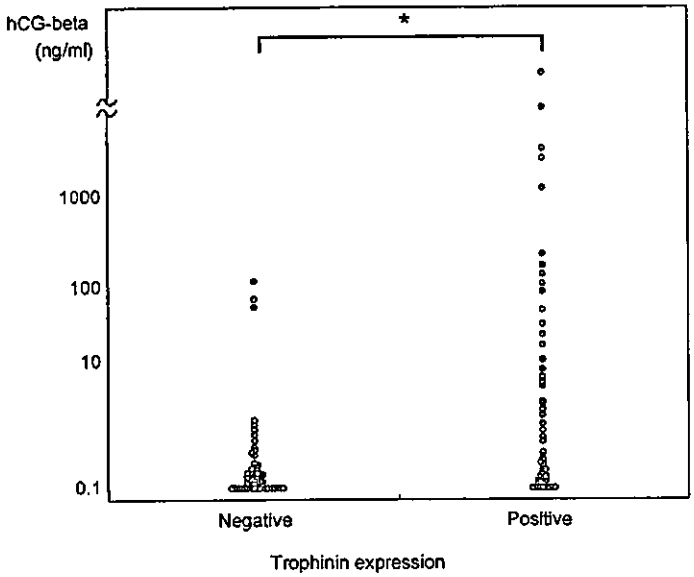

Fig. 1. Correlation between trophinin expression and serum human chorionic gonadotropin (*hCG*)-β concentration. *, statistical significance between trophinin-positive and -negative groups. ($P = 0.004$, Mann-Whitney U test).

the stable transfectants, two clones (JKT-1-Tro-1 and -2) were subjected to tumor assays. As a control cell line, mock-transfectant (vector only) JKT-1-pcDNA1 cells were used.

Flow Cytometric Analysis. JKT-1-Tro cells and mock transfectant cells were assessed by fluorescence-activated cell sorting analysis after incubation with antitrophinin antibody (mouse IgM; Ref. 14) followed by incubation with FITC-conjugated secondary antibodies. Analyses were carried out by FACSort flow cytometry using the CellQuest program (Becton Dickinson).

Growth Rate of Cell Lines. JKT-1-Tro cells and mock-transfectant cells were seeded in 96-well plates at 10^5 cells/ml in α-MEM containing 10% fetal bovine serum and 400 μg/ml of G418 and cultured for various times. The number of living cells was measured each day using the Cell Counting kit (Wako Pure Chemical Industries, Tokyo, Japan). Triplicate cultures were used for each analysis.

Motility and Invasion Assays. A transwell cell culture chamber (Costar, Cambridge, MA) was used for *in vitro* motility and invasion assays with modifications (16). Briefly, the bottom of the upper chamber was sealed with a polyvinylpyrrolidone-free polycarbonate filter with a pore size of 8 nm. The lower face was covered with 50 μg/ml fibronectin (Wako Pure Chemical Industries) in α-MEM medium. Cells (1×10^5) were plated in the upper chamber and incubated in a humidified CO_2 incubator at 37°C for 5 h. The lower chamber was filled with serum-free α-MEM medium. Cells that did not migrate through the membrane were removed, and the cells that migrated to the lower face of the membrane were fixed with methanol followed by Giemsa staining. The number of cells on the lower face was counted under microscope. The mean number of 10 different fields was plotted. For the invasion assay, the upper face of the filter was covered with 100 μg/ml Matrigel (Collaborative Research, Bedford, MA), and the number of cells on the lower face was counted. These assays were carried out in triplicate. The SD of these values was always within 5%.

Orthotopic Tumor Cell Inoculation. BALB/c nude (*nu/nu*) mice, 6–8-week-old males obtained from CLEA Japan, Inc. (Tokyo, Japan), were used for orthotopic tumor cell injection. Mice were anesthetized with avertin, and intratesticular injection was performed. JKT-1-Tro cells (2×10^6) and mock-transfected JKT-1 cells were suspended in 100 μl of serum-free α-MEM and inoculated into the right testis. Three weeks after injection, mice were sacrificed, and testis and other organs having metastasis were removed and fixed with a buffered formalin solution.

Adhesion of JKT-1 Cells to Endothelial Cells. The human pulmonary microvascular endothelial cells (HMVEC-L) were obtained from the Sanko Junyaku Co., Ltd. (Tokyo, Japan) and were cultured in EGM-2M medium containing microvascular endothelial cell growth factors, antimicrobials, and 5% fetal bovine serum to confluence in 24-well culture plate. The wells were washed three times with PBS. JKT-1-Tro cells and JKT-1-mock cells were detached from the plate with trypsin and resuspended in α-MEM (1% fetal bovine serum) and added at 1×10^5 cells/ml on a monolayer of HMVEC-L. For the antibody treatment, JKT-1-Tro cells were incubated with monoclonal antibody against trophinin on ice for 30 min, washed with PBS, and added onto the HMVEC-L monolayer.

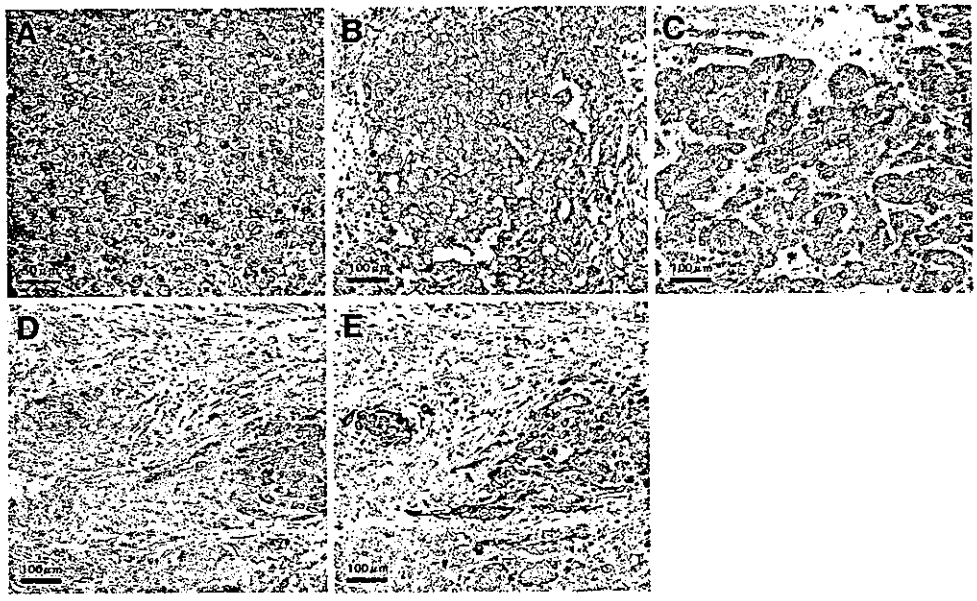

Fig. 2. Immunohistochemistry of human testicular germ cell tumors. Paraffin sections of testicular germ cell tumors were stained with antitrophinin antibody and antihuman chorionic gonadotropin antibody. Each specimen shows seminoma (*A*), embryonal carcinoma (*B*), yolk sac tumor (*C*), and choriocarcinoma (*D–E*). *D* and *E* are serial sections of the same specimen stained with antitrophinin antibody (*D*) and antihuman chorionic gonadotropin antibody (*E*). Counterstaining was performed by hematoxylin.

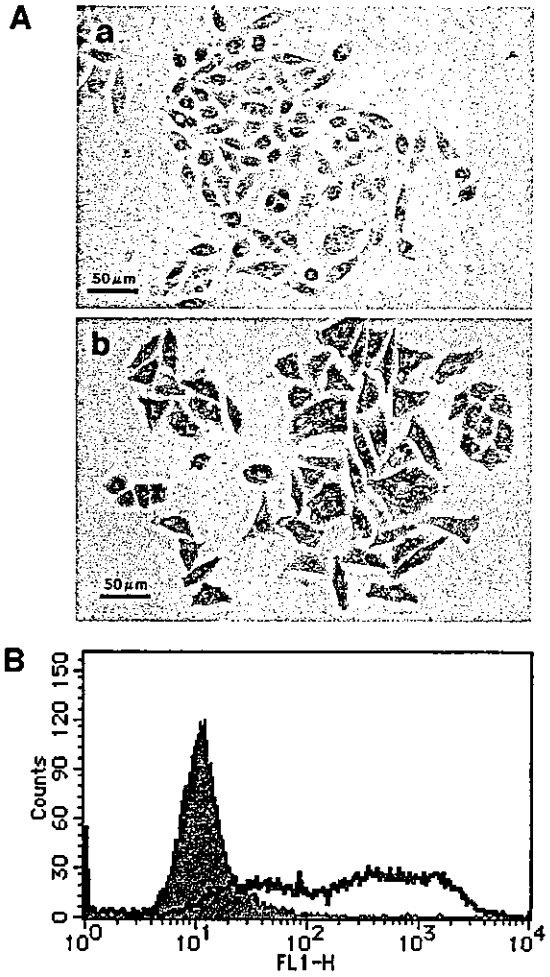

Fig. 3. Expression of trophinin in JKT-1-Tro cells. *A*, fixed but not permeabilized JKT-1 cells were reacted with antitrophinin antibody for detection of trophinin on the cell surface. Note that JKT-1-mock cells (*panel a*) are negative for trophinin, whereas stable transfectant for trophinin, JKT-1-Tro-1 cells (*panel b*) are positively stained with antitrophinin antibody. Another stable transfectant, JKT-1-Tro-2 cells, were also positively stained with antitrophinin antibody with similar intensity (data not shown). *B*, flow cytometry analysis of JKT-1 cells. Cell surface expression of trophinin was confirmed by flow cytometry analysis of intact JKT-1-Tro cells using antitrophinin antibody. JKT-1-Tro-1 cells (*open histogram*) showed higher intensity than mock transfectants (*closed histogram*). JKT-1-Tro-2 cells showed a similar pattern to that of JKT-1-Tro-1 cells (data not shown).

RESULTS

Expression of Trophinin by Patients with Testicular Tumors. Immunohistochemistry of testicular tumors revealed significant positive correlations between trophinin expression and clinical stage (Ref. 17; Table 1). Especially, all of the tumor specimens from patients with lung metastasis were positive for trophinin. Furthermore, serum hCG-β concentration was positively correlated with trophinin expression (Fig. 1), which was confirmed by immunohistochemistry (Fig. 2, *C* and *D*).

We screened 158 patients with testicular tumors. Among them, trophinin was found positive in 39 of 91 (43%) patients in stage I, 14 of 24 (58%) patients in stage II, and 41 of 43 (95%) patients in stage III ($P < 0.001$). Testicular germ cell tumors with stage III were positive strongly for trophinin. Serum hCG concentration was significantly higher in the trophinin-positive group than in the trophinin-negative group (Fig. 1). Remarkably, all of the specimens with lung metastasis were trophinin positive, regardless of seminoma or nonseminomatous germ cell tumor (Table 1). Thus, trophinin expression in the tumor correlates positively with distant metastasis and high levels of serum hCG. These observations suggest that the trophinin-positive testicular tumors are more aggressive than trophinin-negative tumors.

Properties of Trophinin-Positive Seminoma Cell Line, JKT-1-Tro. Because the function of trophinin in cell proliferation and invasion are not known, we investigated whether trophinin plays a role of malignant phenotype in testicular germ cell tumor. Human seminoma cell line JKT-1 does not express trophinin nor trophinin-associated cytoplasmic proteins tastin and bystin (data not shown). JKT-1 cells were transfected with a mammalian expression vector having trophinin cDNA. JKT-1-Tro cells and JKT-1-mock cells obtained by transfection of trophinin cDNA and vector without insert, respectively, were evaluated for their expression of trophinin using antitrophinin antibody by immunocytochemistry (Fig. 3*A*) and flow cytometry (Fig. 3*B*) analysis. Thus, two clones for JKT-1-Tro express trophinin on the

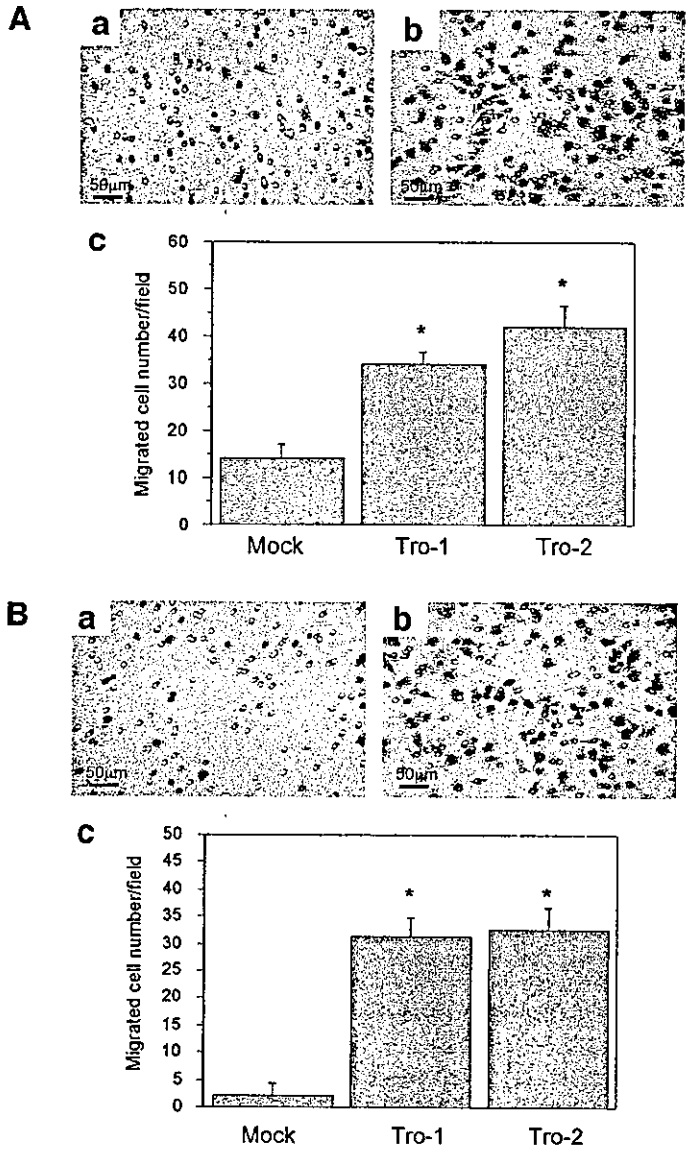

Fig. 4. Motility and invasion activities of JKT-1 cells. Motility and invasion activities of JKT-1 transfectants were assayed by transmigration chambers. *A*, JKT-1-mock cells (*panel a*) and JKT-1-Tro-1 cells (*panel b*) migrated through a filter membrane from uncoated upper chamber to fibronectin coated lower chamber. Cell number count (*panel c*) showed the significant increase of motility of trophinin expressing JKT-1 cells. *, statistical significance against the mock-transfectant cells ($P < 0.001$, Mann-Whitney *U* test). *B*, JKT-1-mock cells (*panel a*) and JKT-1-Tro-1 cells (*panel b*) migrated through Matrigel-coated filter membrane. Invasion potential was significantly increased in JKT-1-Tro cells (*panel c*). *, statistical significance against the mock-transfectant cells ($P < 0.001$, Mann-Whitney *U* test); *bars*, ±SD.